J Solid State Electrochem (2000) 4: 216–224

ORIGINAL PAPER

A.V. Churikov · I.M. Gamayunova · A.V. Shirokov

Ionic processes in solid-electrolyte passivating films on lithium

Received: 22 February 1999 / Accepted: 20 June 1999

Abstract The electrochemical behaviour of a Li electrode in solutions of $LiAlCl_4$ in thionyl chloride, $LiBF_4$ in γ-butyrolactone and $LiClO_4$ in the mixed solvent propylene carbonate (PC) + dimethoxyethane (DME) in the process of cell storage has been investigated by the methods of electrode impedance spectroscopy and pulse voltammetry. Analogous studies have been carried out in PC + DME solution with the Li electrode coated with a specially formed protecting film of Li_2CO_3. The results have been compared with those obtained earlier for other lithium electrochemical systems. The general regularities of the Li electrode electrochemical kinetics attributed to the process of Li^+ ion transport through a passivating film coating a lithium surface have been discussed.

Key words Lithium electrode · Passivating film · Ionic transport · Impedance spectroscopy · Pulse voltammetry

Introduction

The stability of a lithium electrode exposed to a non-aqueous electrolyte solution is well known to be provided by a solid passivating film (PF) formed spontaneously on its surface and presenting a thin continuous layer of insoluble products of metal interaction with the solution components [1–7]. Such a PF is an ionic conductor or solid electrolyte and determines to a great extent the lithium electrode electrochemical behaviour in the electrolyte concentrated solutions, since the kinetics of anodic and cathodic processes are limited by the ion transport in the film [2–7]. A PF is generally recognized to have a complex structure consisting of a dense part in the vicinity of the metal and a porous part exposed to the solution; it is the porousless layer that provides the electrode stability and exerts the greatest resistance to electric current passing.

For describing the structure and electric properties of such a PF, a number of models have been proposed, among which the pioneering ones were the solid electrolyte interphase (SEI) by Peled [2–4] and the polymer electrolyte interphase (PEI) by Thevenin and Garreau [8–10]. The model in most common use is SEI, according to which the passivating films on lithium are considered as a solid electrolyte layer with unipolar cationic conductivity forming immediately after the metal's contact with the environment [2–7]. The initial PF thickness consists of a few nanometres and is capable of enlarging during storage. The limiting stage of the electrochemical reaction is supposed to be the cations' migration through the SEI, and the contributions of metal|film and film|solution interfaces are negligible [3, 4]. The presence of different organic and inorganic compounds in a PF provides its complicated structure that may be conceived as a compositional or multi-layered construction. Proposed later, therefore, were the models of a non-uniform PF combining the SEI and PEI models [11]. Recently, Peled et al. suggested the advanced SEI model, taking into consideration the SEI conductivity via intergrain boundaries [12].

We have also developed a model of ionic processes in solid-electrolyte passivating films on lithium and in similar systems, which is based essentially on the SEI model, but, however, in contrast to the latter, takes into account both the existence of a space-charge region in the solid-electrolyte film at the metal interface and finite duration of ionic carrier transport through the PF [13–18]. The space-charge region occurrence in the solid-electrolyte film at the metal interface is allowed for owing to the appropriate capacitance involvement in the electrode equivalent circuit [17, 18]. A small finite duration of ion transport across a PF comparable to

A.V. Churikov (✉) · I.M. Gamayunova · A.V. Shirokov
Department of Chemistry, Saratov State University,
Astrakhanskaya Str. 83, 410026 Saratov, Russia
e-mail: churikovav@info.sgu.ru
Tel.: +7-8452-516413; Fax: +7-8452-240446

Maxwell dielectric relaxation time leads, at high overpotentials, to the disturbance of electroneutrality in the bulk of the film and to the appearance of space-charge limited currents (SCLCs) [13–16].

A good quantitative agreement of the model theoretical equations with experiment was demonstrated earlier, exemplified by several systems with nonaqueous electrolytes and electrodes made from pure lithium [13, 16, 17], Li-Sn-Cd alloys [15, 18], as well as by a Li electrode incorporated into Li/I_2 current sources [14].

It was of interest to elucidate whether the regularities found are common for lithium electrochemical systems. For this purpose, in the present work the electrochemical behaviour of a lithium electrode in electrolytes based on thionyl chloride (TC), γ-butyrolactone (BL) and propylene carbonate (PC) + dimethoxyethane (DME) in the course of the electrode storage in electrolyte solution has been explored by electrode impedance spectroscopy and pulse galvanostatic methods. The analogous investigations have been carried out using the Li electrode coated with a specially formed protecting film of Li_2CO_3 in the electrolyte based on PC + DME. The validity of the model we proposed earlier for describing the results of these studies has been assessed.

Experimental

The electrochemical measurements were conducted in hermetically sealed glass three-electrode cells containing a few millilitres of electrolyte. The electrodes were made of metallic lithium (99.9%, Mayak, Russia) with the impurities' contents given as: Na, 40 ppm; K, less than 30 ppm; Ca, 75 ppm; Mg, 20 ppm; Al, 30 ppm; N, 30 ppm; Mn, less than 10 ppm. The working electrode was a faced disk electrode obtained by pressing lithium in a glass holder. The electrode surface was formed by cutting off surplus metal before its exposure to the electrolyte solution. The counter electrode was shaped like a cylinder with 12 cm^2 area of internal surface and was manufactured by pressing lithium foil onto a nickel support. The reference electrode was made from lithium wire. All the operations concerned with electrode fabrication, filling with electrolyte solution, assembling and sealing the cells were performed in a glove box in an atmosphere of dry argon (dried by P_2O_5). The assembled cells were stored at 298 $\pm$ 2 K; all the measurements were carried out at 298.0 $\pm$ 0.1 K.

In the present work, the following electrolyte solutions were used: 1 M $LiAlCl_4$ in TC (TC solution), 1 M $LiBF_4$ in BL (BL solution), 1 M $LiClO_4$ in the mixture PC + DME in the ratio of 7:3 (PC + DME solution). The purity of the electrolyte solutions used fulfilled the requirements of lithium battery electrolytes. The TC solution contained impurities: SO_2Cl_2, not more than 0.5 wt%; sulfur chlorides, 30 ppm; Fe, Cr, Cu, Ti, Mo, Ni, less than 1 ppm of each metal. The qualities of the BL solution and the PC + DME solution were characterized by the following parameters: overall alcohol content, less than 0.15%; overall content of other organic impurities, less than 0.15%; H_2O, less than 50 ppm; Na, less than 100 ppm; K, Ca, less than 10 ppm of each metal.

Part of the experiments was performed using the working electrodes coated with a previously formed protecting film of Li_2CO_3. The carbonate film was obtained by annealing the lithium electrodes at 360 K in an atmosphere of dry CO_2. The fact of actual Li_2CO_3 film formation as a result of this procedure was confirmed by analysis of the electrode surface composition using secondary-ion mass spectrometry. The intensities of the mass spectra bands corresponding to the secondary ions derived from Li_2CO_3 (C^+, LiO^+, CO^+, Li_2O^+, O_2^+, Li_3C^+, Li_3O^+, CO_2^+, etc.) increased essentially and regularly in the course of annealing.

The working electrode impedance was measured in the range of frequencies 20 Hz to 200 kHz using a R5021 alternating current bridge; the applied voltage amplitude was 2–5 mV. On $Li|Li_2CO_3$ electrodes the measurements were carried out in the range of frequencies 0.5 Hz to 50 kHz using the fast Fourier transform technique [18]. The measured quantities were adjusted for the impedance values of the cell interelectrode capacitance, for the capacitance and inductivity of current collectors (this correction can be noticeable at high frequencies). Optimal values of the given equivalent circuit parameters were determined by means of computational adjustment reasoning from the condition of minimal discrepancy between the experimental impedance spectrum and the calculated one.

For constructing the polarization current-voltage curve of the electrode under study, the pulse galvanostatic method (method of single rectangular current pulses) was applied, which enables one to avoid the change in the electrode surface state when performing the measurements. The latter were carried out using a PI-50-1 pulse potentiostat with a PR-8 programmer and a G5–56 pulse generator. Potential response was registered by a C9-8 digital memory oscillograph. The ohmic drop in the electrolyte IR_{el} (I is current, R_{el} is electrolyte resistance) was determined from the initial abrupt change in potential. The slope of the initial part of the transient potential-time curve was also involved in evaluating the electrode differential capacitance. At a current pulse duration of 0.5–50 ms the electrode polarization reached approximately constant values, which, after subtracting the IR_{el} drop, were used for constructing polarization curves. The method for constructing the polarization curve of a Li electrode was identical to that described earlier [5, 6, 15]. In all cases the values of polarization measured during forward and backward scanning of the polarization curve were found to coincide. Thus, the charge applied to the electrode in the course of the pulse measurements was sufficiently small and the PF remained undamaged.

Results and discussion

Impedance spectroscopy

Figure 1 shows, in the complex plain, typical impedance Z spectra for the systems under question, registered as a result of their storage under open-circuit conditions. All the spectra are qualitatively similar to each other, as well as to the Li electrode impedance spectra in different organic and inorganic electrolyte systems, the data on which are presented in fairly ample literature dealing with this subject (see, e.g., [8–12, 19–25]). Such spectra are commonly regular or somewhat distorted semicircles with the centre below the real axis. During the process of electrode storage in the electrolyte, spectral characteristic changes are observed, in particular, the semicircle radius enlargement and the frequency diminution in the spectral maximum ω_{max} ($\omega = 2\pi f$ is angular frequency, f is frequency in Hz). The high-frequency intercept value on the real axis determined by spectrum extrapolation is assigned to the resistance R_{el} of the electrolyte solution layer, that is supported by its proportional dependence upon the specific solution conductivity. In the low-frequency region, deviations from an arc are not uncommon. It should be noted that the authors who

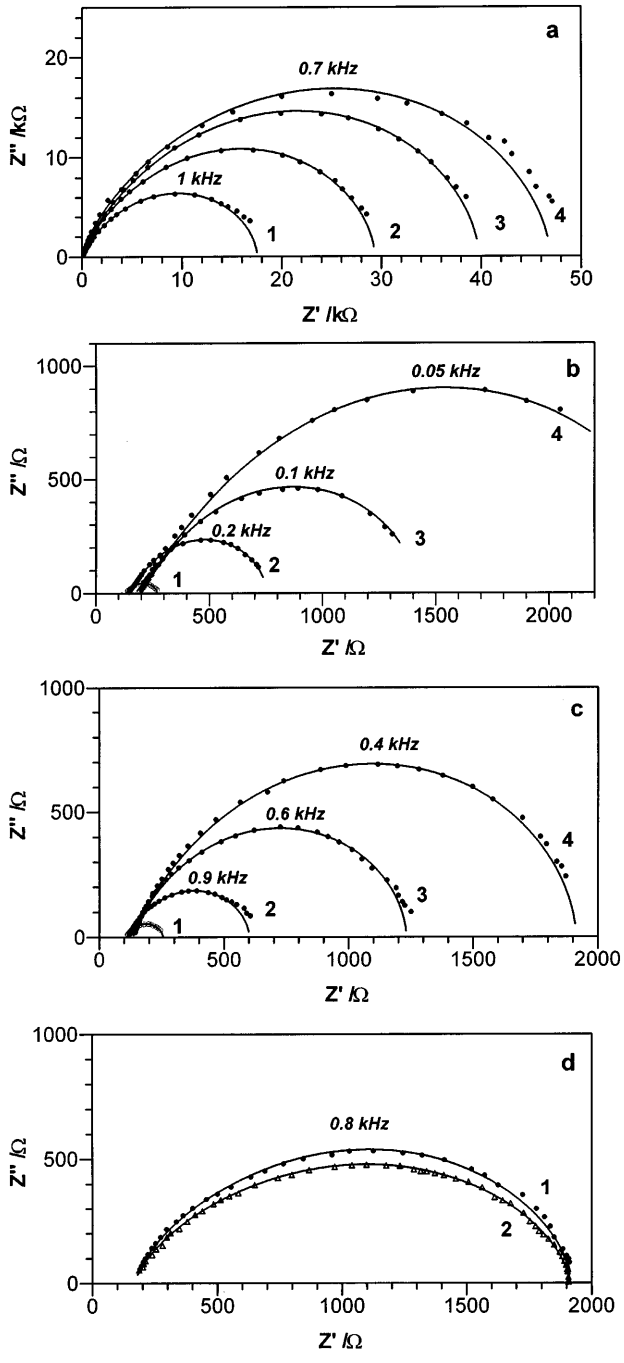

Fig. 1 Impedance spectra of electrochemical systems: **a** Li|1 M $LiAlCl_4$, TC; **b** Li|1 M $LiBF_4$, BL; **c** Li|1 M $LiClO_4$, PC + DME; **d** Li|Li_2CO_3|1 M $LiClO_4$, PC + DME. *Points* mean experiment, *curves* calculation. Duration of cell storage: **a** 1–2 days; 2–8 days; 3–10 days; 4–20 days; **b** 1–2 h; 2–10 days; 3–24 days; 4–128 days; **c** 1–1 h; 2–80 h; 3–46 days, 4–140 days; **d** 1–3 days; 2–84 days. Electrode area **a** 0.06 cm^2 or **b**–**d** 0.07 cm^2. Indicated are the frequencies of the maxima of the curves

explored a frequency range more expanded towards low frequencies sometimes observed a second arc [19, 25].

It is generally accepted trustworthy fact by now that a large arc in the highfrequency region of the Li electrode impedance spectrum has to be attributed to the charge transfer through the PF [8–12, 17–23]. The rate of arc variation reflects the rate of corrosion and relaxation processes occurring in the metal|film|solution structure. The corrosion processes lead to a gradual transformation of a portion of lithium into insoluble corrosion products and to an increase, as a result of that sacrifice, in the PF volume and thickness. The relaxation processes taking place in the PF contemporaneously with its growth cause the PF conducting properties to change owing to its progressive transformation into a state possessing a lower free energy (film recrystallization, defects elimination, etc.).

Among the electrochemical systems discussed here, the PF on Li exposed to BL solution and to the liquid oxidizing agent TC, especially during the few hours just immediately after submerging the electrode in solution, undergoes the fastest change, and the latter is slower in the case of PC + DME solution. In contrast to such films occurring spontaneously, the carbonate film formed artificially on Li by its annealing in CO_2 appears to be fairly stable and to change only slightly when the electrode contacts with the electrolyte (Fig. 1d).

To simulate impedance related to the PF existence, various equivalent circuits have been proposed [4, 8–12, 19–25]. The authors commonly postulate the equivalent circuit construction, reasoning from certain bases, and the coincidence between experimental and calculated impedance spectra serves as a criterion for the circuit applicability for describing the experimental data. However, the simplified equivalent circuits are not appropriate for adequate modelling of Li electrode impedance, whereas the use of complicated equivalent circuits does not lead to unambiguous results on frequent occasions owing to a great number of adjusted parameters. That is why, on choosing the equivalent circuit, the approach based on a preliminary determination of some equivalent circuit elements by means of the spectrum frequency extrapolation seems more reasonable. We intend to use here the equivalent circuit depicted by Fig. 2, which we used earlier for lithium alloys impedance modelling [18]. It includes R_{el}, the geometric capacitance of the passivating film C_{PF}, its ionic resistance R_{PF}, the capacitance of the space-charge region in the PF at the metal interface C_{SC}, and the Warburg impedance Z_W assigned to Li^+ ion diffusion in

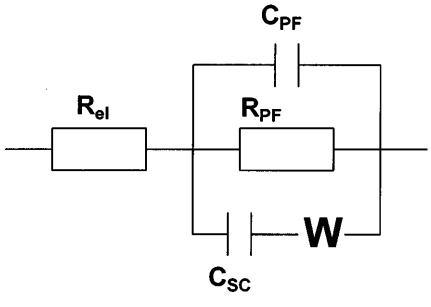

Fig. 2 Simplified equivalent circuit used for modelling the lithium electrode

the film. This circuit could be assumed by means of experimental spectrum analysis, namely by subtracting from the overall impedance both the resistances R_{el} and R_{PF} determined via a common geometric extrapolation in the coordinates Z'–Z'' and the capacitance C_{PF} determined by a geometric extrapolation in the coordinates $1/\omega Z'$–$1/\omega Z''$, and then defining the other elements of the equivalent circuit as was done earlier [17, 18].

The equivalent circuit used here is undoubtedly simplified and does not take into consideration all feasible processes. Nevertheless, it simulates perfectly the impedance spectra for all the electrochemical systems under study within the regions of high and moderately low frequencies, as is shown in Fig. 1 (solid lines). In the low-frequency range ($f < 50$ Hz) the coincidence between computed and experimental spectra is worse, with arc distortions sometimes. This may be related to the diffusion processes in the secondary porous part of the PF, which are not allowed for in the circuit in Fig. 2. At $f > 50$ kHz the interelectrode capacitance should also be included in the equivalent circuit.

Let us introduce the following notations: A is the electrode area; k is the Boltzmann constant; T is the absolute temperature; ε_0 is the dielectric constant of a vacuum; q, n_0, μ and D are the absolute charge, intrinsic bulk concentration, mobility and diffusion coefficient of mobile ions in the film, respectively; ε, σ_0 are the relative dielectric constant and specific ionic conductivity of the PF material, respectively; $i = \sqrt{-1}$. Provided that the thickness of the space-charge region in the PF characterized by the Debye length l_D is much smaller than the thickness L of the solid-electrolyte film itself, so C_{PF} and R_{PF} are defined by routine expressions for a planar-parallel capacitor with leakage:

$$C_{PF} = \frac{\varepsilon\varepsilon_0 A}{L} \tag{1}$$

$$R_{PF} = \frac{L}{\sigma_0 A} = \frac{L}{qn_0\mu A} \tag{2}$$

and the equation for C_{SC} coincides with the corresponding formulae for a differential capacitance of diffuse layer in a 1,1-valent electrolyte or in an intrinsic semiconductor [17, 18]:

$$C_{SC} = \frac{\varepsilon\varepsilon_0 A}{l_D}\cosh\frac{q\Delta\varphi}{2kT} \tag{3}$$

where

$$l_D = \sqrt{\frac{\varepsilon\varepsilon_0 kT}{2q^2 n_0}} \tag{4}$$

$\Delta\varphi$ is the potential drop across the space-charge region. The general Warburg impedance Z_W for diffusion in a finite-length region is defined by the expression:

$$Z_W = \frac{W}{\sqrt{i\omega}}\tanh\left(\sqrt{\frac{i\omega L^2}{D}}\right) \tag{5}$$

where

$$W = \frac{kT}{q^2 n_0 D^{1/2} A} \tag{6}$$

Provided that the above conditions are fulfilled, the following dimensionless combination of the equivalent circuit parameters

$$Y = \frac{(C_{PF}R_{PF})^{1/2}}{C_{SC}W} \tag{7}$$

appears to be dependent solely upon the value of $\Delta\varphi$ according to the formula

$$Y = \frac{1}{\sqrt{2}\cosh\left(\frac{q\Delta\varphi}{2kT}\right)} \tag{8}$$

There is conventionally a regular change of the equivalent circuit parameters with time: R_{PF} and W increase, C_{PF} and C_{SC} decrease. Figure 3 shows the variations during storage for L, σ_0 and Y calculated from these parameters by Eqs. 1, 2 and 7, respectively. When conducting the calculations, the tabulated quantities of the static dielectric constant ($\varepsilon_{Li_2O} = 8.9$; $\varepsilon_{Li_2CO_3} = 4.9$; $\varepsilon_{LiCl} = 10.62$; $\varepsilon_{LiF} = 9.00$) were used. (The principal components of passivating layers forming on lithium in the electrolytes 1 M $LiAlCl_4$, TC and 1 M $LiBF_4$, BL are recognized to be lithium chloride and lithium fluoride, respectively [21, 26–28]. In the PC and PC + DME solutions the PF consists mainly of Li_2O and Li_2CO_3 [7, 29, 30].) Here, along with the other lithium systems, the gain in PF thickness and diminution of its specific conductivity are observed on its aging. A rather slight change in the thickness and conducting properties of the carbonate film is obviously related to preliminary annealing of the electrode and to the high stability of lithium carbonate in the electrolyte. In a number of cases, as Fig. 3a shows, a kinetic curve $L(t)$ becomes a straight line in the coordinates log L-log t, i.e., the PF thickness increase with time obeys the power law $L \sim t^m$ with $m \leq 1$. Of analogous type were also the time dependences of σ_0 (Fig. 3b).

Figure 3c depicts that, for all the systems studied, the Y parameter remains practically unchanged in the course of the PF growth and aging (here presented also are the data for LiSnCd alloys in PC + DME solution taken from [18]). Within the framework of the equivalent circuit interpretation outlined above, the Y constant value means the uniformity of the potential drop $\Delta\varphi$ across the diffuse component of the double electric layer at the metal|PF interface, which could be found from the transformation of Eq. 8:

$$\Delta\varphi = \pm\frac{2kT}{q}\mathrm{Arcosh}\left(\frac{1}{Y\sqrt{2}}\right) \tag{9}$$

For the systems presented in Fig. 3c, estimation of the $\Delta\varphi$ absolute value from Eq. 9 gives the following results: 30 mV, 50 mV and 70 mV for the PF formed on Li in

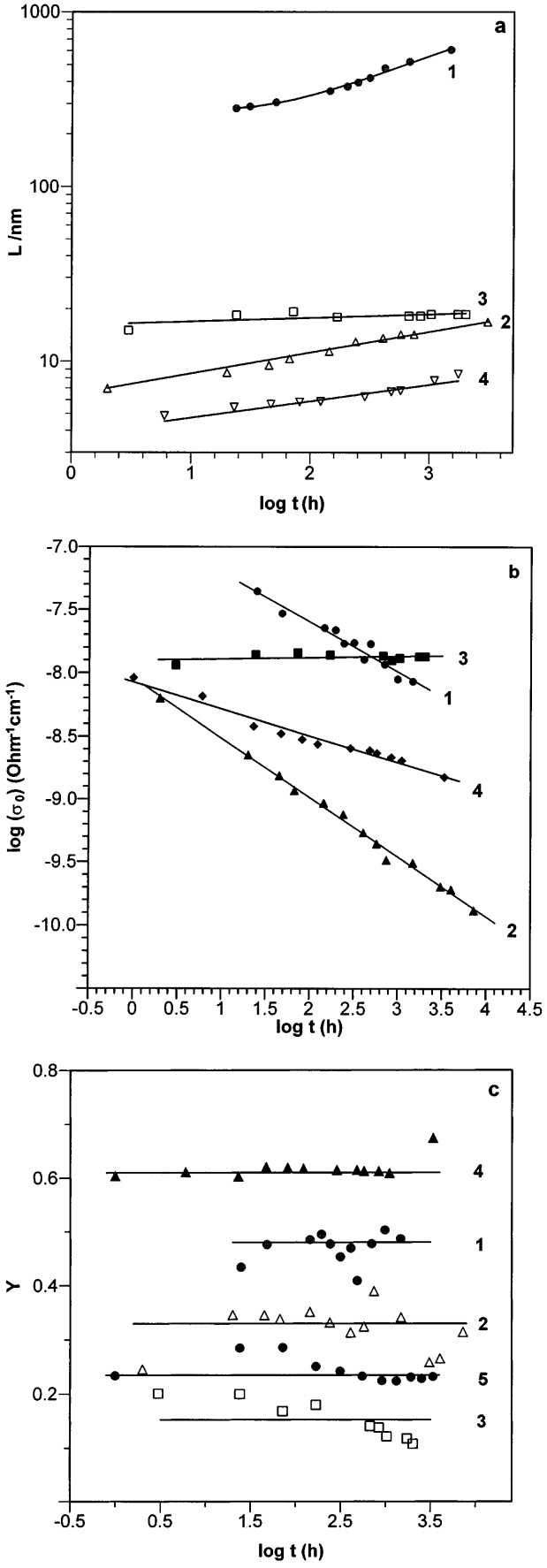

Fig. 3 Changes during storage in **a** L, **b** σ_0 and **c** Y for different electrochemical systems: *1* Li|1 M $LiAlCl_4$, TC; *2* Li|1 M $LiBF_4$, BL; *3* Li|Li_2CO_3|1 M $LiClO_4$, PC + DME; *4* Li|1 M $LiClO_4$, PC + DME; *5* LiSnCd|1 M $LiClO_4$, PC + DME

1 M $LiClO_4$, PC + DME, 1 M $LiAlCl_4$, TC and 1 M $LiBF_4$, BL, respectively; 110 mV for the carbonate film artificially formed on Li in 1 M $LiClO_4$, PC + DME; 90 mV for PF on the alloy LiSnCd in 1 M $LiClO_4$, PC + DME at the equilibrium potentials of these electrodes. It should be noted that the above quantities as themselves are not well reproducible for different electrodes in a series of parallel experiments; nevertheless, the $\Delta\varphi$ value remains usually constant with time for the given object. Within the framework of the Frenkel-Lehovec-Kliewer model [31–33], the $\Delta\varphi$ value is defined, through the energies of defect formation, by the solid as itself, its chemical composition and crystalline structure. Therefore slight variations of the $\Delta\varphi$ value could be explained by the differences in PF formation conditions.

Pulse voltammetry

Figure 4 depicts the typical polarization current-voltage curves in the coordinates log j-log η as the dependences of current density j upon overpotential η for the electrodes made from pure lithium in the PC + DME solution and BL solution. The j-η curves are constructed by separate points registered using the pulse method (see Experimental). Earlier, such forms for the j-η curves were demonstrated by the examples of Li electrodes in PC solutions and for the Li-Sn-Cd system electrodes in PC + DME solutions [13, 15]. The anodic and cathodic components of the polarization curve are symmetric with respect to zero, so only the anodic ones are presented in the graphs. For all the lithium electrochemical systems listed above, the experimental j-η curves obey the following equation closely:

$$j = \frac{qn_0\mu\eta}{L} + \lambda\frac{\mu\varepsilon\varepsilon_0\eta^2}{L^3} \tag{10}$$

which can also be written in another form:

$$j = \frac{\sigma_0\eta}{L}\left(1 + \lambda\frac{\eta}{\eta_0}\right) \tag{11}$$

where

$$\eta_0 = \frac{qn_0L^2}{\varepsilon\varepsilon_0} \tag{12}$$

and λ is a dimensionless coefficient adopting the values from 1/2 to 9/8 on the overpotential change from zero to infinity and being quite well approximated by the equation

$$\lambda = 0.5 + \frac{(\eta/\eta_0)^a}{b + 1.6(\eta/\eta_0)^a} \tag{13}$$

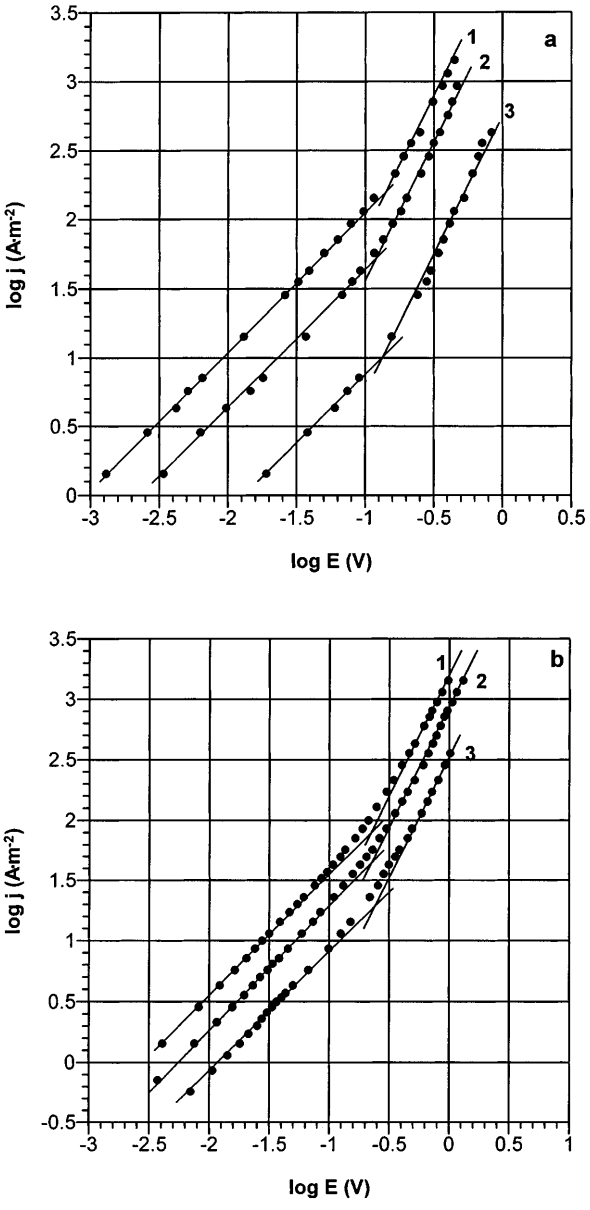

Fig. 4 Polarization curves for the systems **a** Li|1 M $LiBF_4$, BL and **b** Li|1 M $LiClO_4$, PC + DME. Duration of electrode contact with electrolyte: **a** 1–2 h, 2–3 days, 3–62 days; **b** 1–1 day, 2–20 days, 3–140 days. *Straight lines* are presented with slopes equal to 1 and 2

with $a = 1.25$ and $b = 0.7729$. Another somewhat more unwieldy expression approximating the dependence of λ on η has been proposed [13].

Equation 10 was deduced earlier [15, 16] within the framework of the SCLC model, reasoning from the following suppositions: (1) the PF is a thin, poorly conducting layer with unipolar cationic conductivity positioned between two phases with high conductivity; (2) the mobile ionic carriers concentration in the bulk of the PF, n_0, is much more lower than the carriers concentration at the metal|PF and PF|solution interfaces; thus the concentrations at the interfaces could be assumed to be infinitely great and the contacts themselves to be ohmic and lacking any potential drop, the latter totally occurring in the bulk of the film; (3) the potential drop across the film leads to injecting, from the contact into the film, of cations a type like the intrinsic PF carriers; (4) the distribution of both the electric potential and ion concentration in the PF obeys the Poisson equation and the equation of continuous current. Under these conditions, Eq. 10 or 11 describes a voltage-current curve of the metal|film|solution system [15].

One can believe that Eq. 11 deals essentially with the gain in specific ionic conductivity σ up to its own value σ_0 on current flowing. This increase is especially notable when η becomes comparable to some characteristic overpotential η_0. The film conductivity increases owing to the greater concentration of mobile charges in it. We do not consider the definite microscopic mechanisms of charge transfer, about which reliable data are absent with respect to a PF on Li.

A physical reason for the appearance of excess ions space-charge in the PF is the fact that owing to a very small thickness of the PF, the duration of transport across it (equal to $t_0 = 4L^2/(3\ \mu\eta)$ [34]) of the carriers injected from the electrode appears, at a definite potential difference, less than the Maxwell dielectric relaxation time ($t_M = \varepsilon\varepsilon_0/\sigma_0$), which in its turn is sufficiently great owing to the low specific electroconductivity of the PF. This means the occurrence of conditions under which the non-equilibrium charge has not enough time to "disappear" during its transport from one film boundary to another, which causes the disturbance in the PF bulk electroneutrality on current flowing. It follows from the equality $t_0 = t_M$ that a transition from ohmic current mode to an injection one takes place at the polarization $\eta^* = 4\eta_0/3$. Equation 12 shows that the necessary polarization value η^* declines rapidly with the decrease in layer thickness L. It is not inconceivable that the above fact is just the reason for the possibility to observe the injection currents in the electrochemical systems with a lithium electrode coated by a passivating film, since such film thicknesses are rather small (from 1 to 1000 nm).

The polarization curves presented in Fig. 4 in the coordinates log j-log η obey Eq. 10. Indeed, the straight lines with a slope equal to 1 transform into lines with a slope of 2, i.e. a current proportionality to overpotential gives way to that with overpotential squared on current increase. The straight lines with unity slope at low polarizations (Ohm's law) are assigned to the region of intrinsic ionic conductivity of the PF and are described by the first summand of Eq. 10, whereas the straight lines with the slope of 2 correspond to the region of PF electroconductivity growth due to non-equilibrium carrier injection on sufficiently high polarization and are described by the second summand of Eq. 10. Poor dependence of the λ coefficient upon ς does not violate appreciably the $j \sim \eta^2$ law.

The same situation takes place in Fig. 5, where the analogous j-η curves in the range of great η for the Li

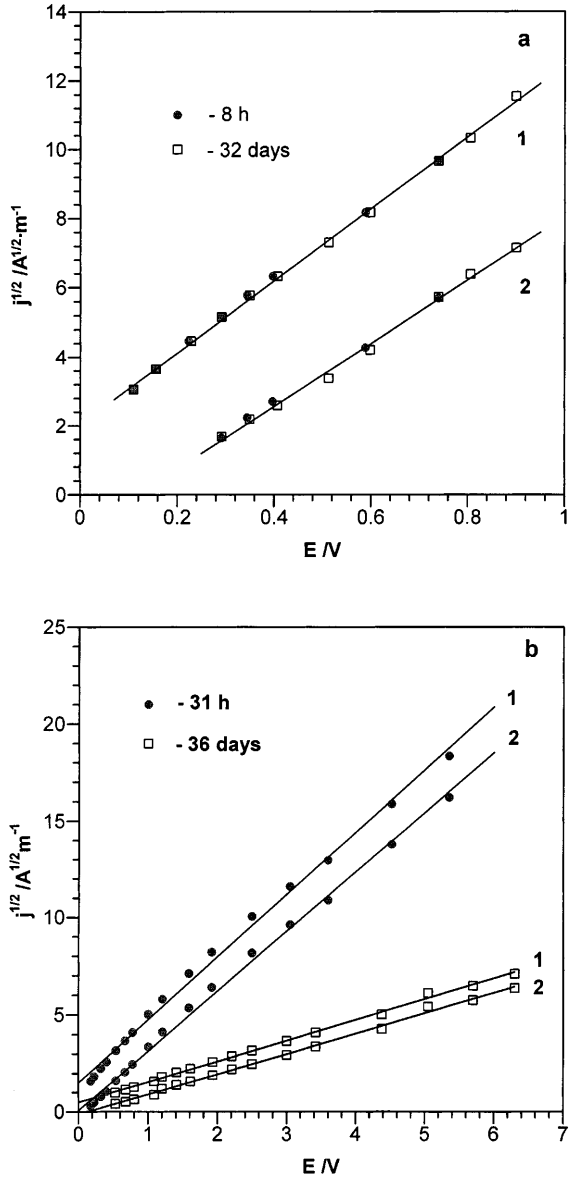

Fig. 5 Polarization curves for overall (*1*) and injection (*2*) currents; systems **a** $Li|Li_2CO_3|1\ M\ LiClO_4$, PC + DME and **b** Li|1 M $LiAlCl_4$, TC. Storage duration is indicated on the figure

electrode in TC solution, as well as for the lithium electrode coated with the artificial Li_2CO_3 film in the PC + DME solution, are depicted in the coordinates $\sqrt{j} - \eta$ and $\sqrt{j_{inj}} - \eta$ (j_{inj} is injection current defined as the difference between the overall current j and the linear ohmic current, and described by the second summand of Eq. 10. The square law is fulfilled for both the injection and overall currents, the angular coefficients of the corresponding $\sqrt{j} - \eta$ and $\sqrt{j_{inj}} - \eta$ straight lines being the same. As follows from Eq. 10, the slope of these lines is near $\sqrt{9\mu\epsilon\epsilon_0/(8L^3)}$, since in the square region the coefficient λ is close to its upper limit of 9/8. Thus, the ion mobility μ can be calculated from the slope of the straight line portions of the $\sqrt{j} - \eta$ dependences.

The lithium electrode polarization curves do not undergo qualitative changes during storage of the electrode|solution system. The quantitative alterations in the characteristics, as well as the impedance spectra evolution, are caused by the corrosion and relaxation processes occurring in the PF. The rates of these processes (involved in the systems under consideration) are maximal for the PF in BL and TC solutions and minimal for Li_2CO_3 films, as is reflected by Figs. 4 and 5.

Computations processing the experimental j-η curve using Eq. 10 or 11 enable us to calculate two of the constants included in the equations provided that the others are known. Applying the computational fitting, we determined the optimal values of μ and n_0, which serve in the given case as the adjusted parameters, while q, L and ε are considered as known constants. The PF thicknesses were calculated from the C_{PF} values by Eq. 1.

The μ and n_0 values for a PF formed in BL solution were of the same order as the corresponding values calculated for a PF in PC + DME solution and varied in the same manner during the electrode aging in the solution: the carrier mobility remained approximately unchanged, whereas the carrier concentration diminished by about 5–10 times during the first month of storage. For a PF in BL solution, such changes take place at a higher rate and are more pronounced. Such character of the time dependences of μ and n_0 is valid in the series of concurrent experiments. As for the special numerical values of the μ and n_0 calculated parameters, a certain spread in them was observed from one electrode to another, which is a common phenomenon for lithium electrochemical systems. On computer processing the polarization curves shown in Fig. 4, which were chosen by us as typical, μ values equal to 2×10^{-7} $cm^2\ V^{-1}\ s^{-1}$ for a PF in BL solution and 3×10^{-8} $cm^2\ V^{-1}\ s^{-1}$ for a PF in PC + DME solution were obtained. The corresponding n_0 values changed during 2 months of storage from 4×10^{18} to 2×10^{17} cm^{-3} for a PF formed in BL solution, and from 1×10^{19} to 2×10^{18} cm^{-3} for a PF formed in PC + DME solution. The orders of magnitude seem to be reasonable, having regard to the fact that PFs on Li are polycrystalline objects with conductivity predominately via the grain boundaries [12, 13]. However, the measurements carried out during the first hours of cell storage with BL solution were not governed by this regularity on frequent occasions, that may be related to a chemical transformation of oxide-hydroxide-carbonate impurities in LiF deposited on the lithium surface [27, 28]. A peculiar kind of this effect was also observed for a PF on Li in TC solution, where during the initial hours of electrode storage in solution the calculated mobility of the carriers increased from 2×10^{-7} to 3×10^{-6} $cm^2\ V^{-1}\ s^{-1}$ and then remained approximately constant [13]. The carrier concentration over 2 months of electrode storage in TC solution decreased from 2×10^{18} to 1×10^{16} cm^{-3}. During the same time the parameters μ and n_0 for Li_2CO_3 film formed by annealing were essentially unchanged, remaining equal to 1×10^{-7} $cm^2\ V^{-1}\ s^{-1}$ and 1×10^{18} cm^{-3}, respectively.

These values apparently correspond to a stationary state of the film after annealing.

Attention must be given also to agreement between the data on PF electrophysical characteristics obtained by alternating and direct current measurements. Thus, the $n_0\sqrt{D}$ values can be calculated from either the Warburg constant by Eq. 6, or the values n_0 and μ using the Nernst-Einstein relationship $\mu = qD/kT$. For the systems under consideration they are presented in Fig. 6. As indicated by the figure, the $n_0\sqrt{D}$ quantities determined from replicate impedance and polarization measurements are of the same order of magnitude and change in the same manner with time. This is also valid for the ratio l_D/L, which could be calculated by means of Eq. 3 or 4 using the values $\Delta\varphi$, C_{PF} or n_0, respectively. For the different systems studied, the ratio l_D/L was within the range of 0.05–0.25. Nevertheless, a complete matching of curves was not observed on frequent occasions. The explanation may be a somewhat simplified character of the models under discussion, in particular, neglect of the multi-layered structure of the PF dense component and of its non-uniform properties with respect to thickness [7, 12, 23, 27, 28]. Besides, there is some uncertainty for the L measurements, since it is known that different methods result in different values of the PF thickness [7]. That is why the n_0 and μ values presented here must be regarded as rather rough assessments.

We used in our calculations the tabulated values of macroscopic dielectric constants, whilst those may differ for PFs that are non-homogeneous in structure and density. Furthermore, the properties of very thin films do not coincide with those of bulk material. That is why it seems reasonable to demonstrate the changes in calculated parameters provided that another ε value (and, therefore, L, since we calculate the PF thickness by Eq. 1) is assumed. On increasing ε by N times, the same gains in L, σ_0, as well as l_D taken from the Eq. 3 or 4 occur, whereas μ values defined by Eq. 10 increase by N^2 times, and n_0 decreases by N times. This leads to a parallel shift of lines in Fig. 3a, b, while Fig. 3c and Fig. 6 remain unchanged. The situation when ε is a function of the coordinate is more complicated and not within the framework of the model under question.

Attention must also be paid to the following circumstance. The SCLC phenomenon is well known for electronic carriers [34], whereas the ionic SCLCs are observed much more rarely (e.g. [35–39]), so, in general, evidence is necessary for defining the nature of the current carriers. While the ionic nature of the current in a PF on Li at low overpotentials is beyond question, since the charge transport is accompanied by the metal dissolving-precipitating, there are no direct data on the nature of the carriers with respect to currents flowing at high polarizations. Therefore, in principle, another interpretation is possible for the j-η curves in the present work, namely that at high overpotentials the conditions for electronic carrier injection from contacts into the PF are realized. To put it otherwise, electronic SCLCs interfere with the intrinsic conductivity of the PF. Under these circumstances the calculated μ values should be assigned to electronic carriers, but the concentration and mobility of the ions could not be determined from the j-η curves. Reasoning from these remarks, the conformity between the data obtained from impedance measurements within the range close to the electrode equilibrium potential, and the data from current-voltage measurements at great deviations from equilibrium, confirms the identical nature of the current carriers in both cases.

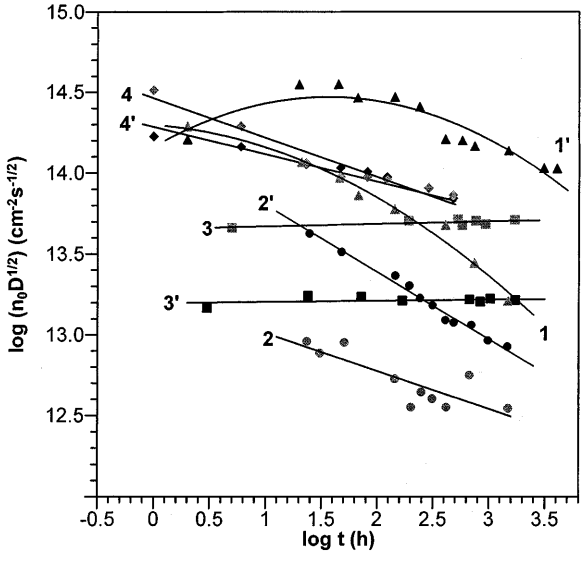

Fig. 6 Time dependences of $n_0\sqrt{D}$ values calculated from polarization characteristics (*1*, *2*, *3*, *4*) and from impedance spectra (*1′*, *2′*, *3′*, *4′*) for different electrochemical systems: *1,1′* Li|1 M $LiBF_4$, BL; *2,2′* Li|1 M $LiAlCl_4$, TC; *3,3′* Li|Li_2CO_3|1 M $LiClO_4$, PC + DME; *4,4′* Li|1 M $LiClO_4$, PC + DME

Conclusion

Using the methods of electrode impedance spectroscopy and pulse voltammetry, ionic processes in solid-electrolyte passivating films on a lithium surface in various nonaqueous electrolyte solutions have been explored. Different lithium electrochemical systems have been established to show analogous electrochemical behaviour assigned to ionic transport processes in PFs. The applicability of the model we proposed earlier for ionic processes in PFs on Li and similar systems [13–18], which takes into consideration both the occurrence of the space-charge region in the solid-electrolyte film at the metal interface and a finite duration of the ionic carrier transport through the PF, has been estimated for describing the results of these studies. The space-charge region existence in PFs at the metal interface is accounted for by means of the corresponding capacitance involvement in the electrode equivalent circuit. A short finite time for ionic transport across the PF comparable to the Maxwell dielectric relaxation time leads, at high

overpotentials, to the disturbance of the bulk film electroneutrality and to the flow of space-charge limited currents. It may be concluded in general that the experimental data are in good agreement with this model, and that the views developed earlier on the mechanism and regularities of the electrochemical processes occurring on the Li electrode coated with a passivating film could be extended over the majority of such systems.

Acknowledgements The authors are grateful to the Russian Foundation for Basic Research (projects no. 97-03-32619 and no. 99-03-32320) for the financial support of the present work.

References

1. Dey AN (1977) Thin Solid Films 43: 131
2. Peled E, Yamin H (1979) Isr J Chem 18: 131
3. Peled E (1979) J Electrochem Soc 126: 2047
4. Peled E (1983) Lithium stability and film formation in organic and inorganic electrolyte for lithium battery systems. In: Gabano JP (ed) Lithium batteries. Academic Press, New York, p 43
5. Moshtev RV, Geronov Y, Puresheva B (1981) J Electrochem Soc 128: 1851
6. Geronov Y, Schwager F, Muller RH (1982) J Electrochem Soc 129: 1422
7. Schwager F, Geronov Y, Muller RH (1985) J Electrochem Soc 132: 285
8. Garreau M, Thevenin J, Milandou B (1984) In: Dey AN (ed) Proceedings of the symposium on lithium batteries, Washington. Electrochemical Society, Pennington, NJ, p 28
9. Thevenin JG (1985) J Power Sources 14: 45
10. Garreau M (1987) J Power Sources 20: 9
11. Thevenin JG, Muller RH (1987) J Electrochem Soc 134: 273
12. Peled E, Golodnitsky D, Ardel G (1997) J Electrochem Soc 144: L208
13. Nimon ES, Churikov AV, Shirokov AV, Lvov AL, Chuvashkin AN (1993) J Power Sources 44: 365
14. Nimon ES, Shirokov AV, Kovynev NP, Lvov AL, Pridatko IA (1995) J Power Sources 55: 177
15. Nimon ES, Churikov AV (1996) Electrochim Acta 41: 1455
16. Churikov AV, Nimon ES, Lvov AL (1998) Russ J Electrochem 34: 669
17. Churikov AV, Lvov AL (1998) Russ J Electrochem 34: 662
18. Churikov AV, Nimon ES, Lvov AL (1997) Electrochim Acta 42: 179
19. Moshtev RV, Puresheva B (1984) J Electroanal Chem 180: 609
20. Gaberšček M, Jamnic J, Pejovnik S (1989) J Power Sources 25: 123
21. Zhang Y, Cha C (1992) Electrochim Acta 37: 1211
22. Popov BN, Zhang W, Darcy EC, White RE (1993) J Electrochem Soc 140: 3097
23. Aurbach D, Zaban A, Gofer Y, Abramson O, Ben-Zion M (1995) J Electrochem Soc 142: 687
24. Aubay M, Lojou E (1994) J Electrochem Soc 141: 865
25. Takami N, Ohsaki T, Inada K (1992) J Electrochem Soc 139: 1849
26. Kovač M, Milićev, Kovač A, Pejovnic S (1995) J Electrochem Soc 142: 1390
27. Kanamura K, Tamura H, Shiraishi S, Takehara Z (1995) J Electrochem Soc 142: 340
28. Kanamura K, Tamura H, Shiraishi S, Takehara Z (1995) Electrochim Acta 40: 913
29. Aurbach D, Gofer Y, Langzam J (1989) J Electrochem Soc 136: 3198
30. Aurbach D, Gofer Y (1991) J Electrochem Soc 138: 3529
31. Frenkel J (1946) Kinetic theory of liquids. Oxford University Press, New York
32. Lehovec K (1953) J Chem Phys 21: 1123
33. Kliewer KL, Koehler JS (1965) Phys Rev 140: A1226
34. Lampert MA, Mark P (1970) Current injection in solids. Academic Press, New York
35. Hofstein SR (1967) Appl Phys Lett 10: 291
36. Tödheide-Haupt U, Gysler A, Ruppel W (1966) Phys Stat Solidi 15: 567
37. Engelhardt H, Riehl N (1965) Phys Lett 14: 20
38. Faughnan BW, Crandall RS, Lampert MA (1975) Appl Phys Lett 27: 275
39. Kluger K, Lohrengel MM (1991) Ber Bunsenges Phys Chem 95: 1458